

AD-A190 860

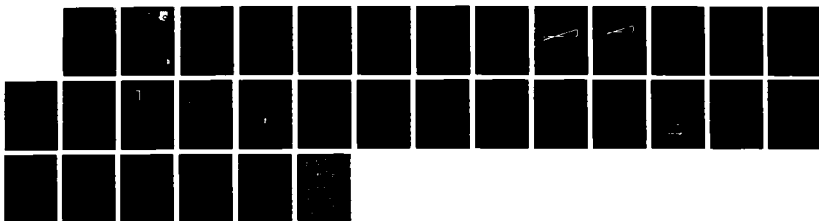
GENERATION OF TUNABLE COHERENT RADIATION IN 3
MICROMETERS-5 MICROMETERS R. (U) TACAM CORP CARLSBAD CA
H M SALOUR NOV 87 AFMAL-TR-87-2075 F33615-85-C-2565

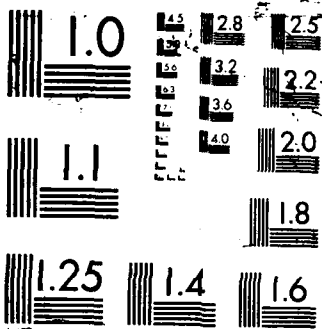
1/1

UNCLASSIFIED

F/G 9/3

NL





AD-A190 860

AFWAL-TR-87-2075

GENERATION OF TUNABLE COHERENT RADIATION
IN 3 μm - 5 μm REGION USING SEMICONDUCTOR LASERS
IN EXTERNAL CAVITIES

Michael M. Salour

TACAN CORPORATION
2111 PALOMAR AIRPORT ROAD
CARLSBAD, CALIFORNIA 92009

4 NOVEMBER 1987

FINAL REPORT FOR PERIOD AUGUST 1985 - JULY 1986

APPROVED FOR PUBLIC RELEASE; DISTRIBUTION UNLIMITED.

AERO PROPULSION LABORATORY
AIR FORCE WRIGHT AERONAUTICAL LABORATORIES
AIR FORCE SYSTEMS COMMAND
WRIGHT-PATTERSON AIR FORCE BASE, OHIO 45433-6563

DTIC FILE COPY



DTIC
ELECTE
FEB 02 1988
S
D
C
E

88 1 28 074

Unclassified

SECURITY CLASSIFICATION OF THIS PAGE

REPORT DOCUMENTATION PAGE

1a. REPORT SECURITY CLASSIFICATION Unclassified			1b. RESTRICTIVE MARKINGS None			
2a. SECURITY CLASSIFICATION AUTHORITY N/A Since Unclassified			3. DISTRIBUTION/AVAILABILITY OF REPORT approved for public release; distribution is unlimited			
2b. DECLASSIFICATION/DOWNGRADING SCHEDULE N/A Since Unclassified						
4. PERFORMING ORGANIZATION REPORT NUMBER(S)			5. MONITORING ORGANIZATION REPORT NUMBER(S) AFWAL-TR-87-2075			
6a. NAME OF PERFORMING ORGANIZATION TACAN Corporation		6b. OFFICE SYMBOL (If applicable)	7a. NAME OF MONITORING ORGANIZATION Aero Propulsion Lab (AFWAL/POOC) Air Force Wright Aeronautical Laboratories			
6c. ADDRESS (City, State and ZIP Code) 2111 Palomar Airport Road, #270 Carlsbad, CA 92009			7b. ADDRESS (City, State and ZIP Code) Wright-Patterson AFB, OH 45433-6563			
8a. NAME OF FUNDING/SPONSORING ORGANIZATION Aero Propulsion Laboratory		8b. OFFICE SYMBOL (If applicable) AFWAL/POOC	9. PROCUREMENT INSTRUMENT IDENTIFICATION NUMBER F33615-85-C-2565			
8c. ADDRESS (City, State and ZIP Code) Air Force Wright Aeronautical Laboratories Air Force Systems Command Wright-Patterson AFB, OH 45433-6563			10. SOURCE OF FUNDING NOS.			
			PROGRAM ELEMENT NO. 61102F	PROJECT NO. 2301	TASK NO. S1	WORK UNIT NO. 29
11. TITLE (Include Security Classification) Generation of Tunable Coherent Radiation in 3 μm - 5 μm Region Using Semiconductor Lasers in External Cavities						
12. PERSONAL AUTHOR(S) SALOUR, Michael M.						
13a. TYPE OF REPORT Final Report		13b. TIME COVERED FROM 85 08 TO 86 07		14. DATE OF REPORT (Yr., Mo., Day) 1987 November		
15. PAGE COUNT 31						
16. SUPPLEMENTARY NOTATION						
17. COSATI CODES			18. SUBJECT TERMS (Continue on reverse if necessary and identify by block number)			
FIELD	GROUP	SUB. GR.	Tunable Infrared Semiconductor Lasers in the 3 μm to 5 μm region, Lead Sulfide, Se pn-junction			
19. ABSTRACT (Continue on reverse if necessary and identify by block number)						
<p>This report describes the first optically pumped mode-locked $\text{PbS}_{1-x}\text{Se}_x$ semiconductor lasers with an external cavity with the following specifications:</p> <ol style="list-style-type: none"> 1. Observed lasing as high as to 150K, 2. Operated CW mode-locked as low as temperature of 8K, 3. Maximum output average power was 1 mW at 4.1 μm and 0.6 mw at 4.8 μm, 4. Wavelength span from 4 μm - 5 μm possible. 						
20. DISTRIBUTION/AVAILABILITY OF ABSTRACT UNCLASSIFIED/UNLIMITED <input checked="" type="checkbox"/> SAME AS RPT. <input type="checkbox"/> NOTIC USERS <input type="checkbox"/>			21. ABSTRACT SECURITY CLASSIFICATION Unclassified			
22a. NAME OF RESPONSIBLE INDIVIDUAL B.N. Ganguly			22b. TELEPHONE NUMBER (Include Area Code) 513-255-2923		22c. OFFICE SYMBOL AFWAL/POOC-3	

PREFACE

The authors wish to thank Dr. K. Vilhelmsson, Dr. B. Valk, Mr. E.L. Mason and Mr. D.J. Olson for technical assistance. This work was supported by the Aero Propulsion Laboratory, Air Force Wright Aeronautical Laboratories, Air Force Systems Command, Wright-Patterson AFB, OH 45433-6563.

Accession For	
NTIS GRA&I	<input checked="" type="checkbox"/>
DTIC TAB	<input type="checkbox"/>
Unannounced	<input type="checkbox"/>
Justification	
By	
Distribution/	
Availability Codes	
Dist	Avail and/or Special
A-1	



TABLE OF CONTENTS

<u>SECTION</u>	<u>PAGE</u>
I. INTRODUCTION	1
1. Optical Pumping in Semiconductors Involving External Cavities	1
II. DESIGN DETAILS	7
1. Crystal Gain Media	7
2. CW and Pulsed Operation of the $\text{PbS}_{1-x}\text{Se}_x$ Laser Under a Variety of Pumping Configurations and Sources.	13
3. Experimental Setup	19
4. Experimental Results	20
III. CONCLUSIONS	24
REFERENCES	25

LIST OF FIGURES

FIGURE	TITLE	PAGE
1	Semiconductor Ring Laser	3
2	Semiconductor Ring Laser With Optical Diode	4
3	Schematic Diagram of Graded Structure	8
4	Stacked Array of Crystals	8
5	Continuously Varied Bandgap	10
6	Longitudinally Pumped Variation	10
7	Lyot Filters for Frequency Selective Elements	11
8	Transverse Pumping	12
9	Experimental Setup of Pulse Chirping	18
10	Experimental Configuration	19
11	Input-Output Power Characteristics at a Cold Finger Temperature of 8 K	20
12	Spectral Characteristics at 200 mW Input Average Power	22

I. INTRODUCTION

This work explored a variety of novel designs and concepts in the generation of tunable coherent radiation in the 3- μ m to 5- μ m region of the electromagnetic spectra. This research was a direct result of earlier work which led to the first successful invention of an optically pumped semiconductor laser in external cavities. Processes that were studied include the following:

1. Construction of an optically pumped tunable ring semiconductor $\text{PbS}_{1-x}\text{Se}_x$ platelet laser operating in the 3- μ m to 5- μ m region of the electromagnetic spectra.
2. Study of a CW and pulsed operations of the cavity under a variety of pumping configurations and sources.
3. Study of complete tunability in the 3- μ m to 5- μ m range utilizing graded bandgap crystal arrays.
4. Exploration of room temperature operation, utilizing superlattice structure.
5. Study of the overall system efficiency as a function of the cavity design, operating wavelength, mode discipline, method of pumping and the gain medium.

Some potential applications of the recently completed work include infrared communications, spectroscopy, and the testing of infrared optical fibers.

1. OPTICAL PUMPING IN SEMICONDUCTORS INVOLVING EXTERNAL CAVITIES

Optical pumping of semiconductors has the advantage over diode and dye lasers in that virtually any direct bandgap semiconductor can be used, thereby increasing the available spectral range. Recently mode-locked laser action in external cavity of synchronously pumped semiconductor materials like CdS, CdSe, InGaAsP , and HgCdTe has been demonstrated in the wavelength range 0.49 to 2 μm .^[13,17,23-25] Mode-locked lasing of thick GaAs bulk crystals has also been observed using a two-photon synchronous pumping configuration.^[26] These lasers have advantages over dye lasers because of the lack of dye instability in the infrared and in addition no jet fluctuations are present, eliminating a very strong source of noise, and they can be operated completely in vacuum. Furthermore, the spontaneous spectrum is narrower than those of dyes, allowing a stabilized single-frequency laser to operate with fewer wavelength selective elements,

while tuning can be done by varying the temperature. However, the wavelength range spanning from 0.49 to 2 μm is not yet covered completely by mode-locked semiconductor lasers due to the lack of available high quality semiconductor materials in platelet form of any desired composition.

We report here the development of a cw mode-locked $\text{PbS}_{1-x}\text{Se}_x$ semiconductor platelet laser whose output frequency and power characteristics provide an attractive tunable source in the near infrared. The laser reported here has the advantage of high beam quality and high output powers compared with other semiconductor lasers operating in the visible spectral range.

a. Optically Pumped Tunable Ring Semiconductor $\text{PbS}_{1-x}\text{Se}_x$ Platelet Laser Operating in the $3\mu\text{m}$ to $5\mu\text{m}$ Region of the Electromagnetic Spectra

(1) Design Consideration for the Master Oscillator--The successful demonstration of the optically pumped semiconductor laser in external ring cavity has created a great enthusiasm in the laser community. These lasers combine the advantage of an increased spectral range over dye lasers with the possibility of intracavity tuning elements not available in diode lasers. Ring dye lasers have resulted in increased single-frequency output power^[1] and for research, an optically pumped semiconductor laser in a ring cavity configuration as a master oscillator was constructed.

The active medium utilized was a platelet ($\sim 30 \mu\text{m}$ thick) of $\text{PbS}_{1-x}\text{Se}_x$ mounted onto a piece of optical quality sapphire (Figure 1). The sapphire has its axes parallel to the axes of the platelet to prevent depolarization of the laser beam. The sapphire was mounted on a copper frame attached to a liquid-nitrogen chamber to maintain a sample temperature of 85K. The Nd:YAG laser pump beam at $1.06\mu\text{m}$ is focused to a spot size of $\sim 5 \mu\text{m}$ through the window of the dewar using a 10X microscope objective which also serves to collimate the crystal fluorescence. The same type of microscope objective was used at the backside of the dewar to collimate the rear fluorescence. The windows of the dewar, as well as the backside of the sapphire, were (single-layer) anti-reflection (AR) coated. Mirrors M_2 , M_3 , and M_4 were flat and highly reflective, while the flat mirrors used as output mirror M_1 had transmissions between 0.5 percent and 50 percent. A polarizing beamsplitter distinguished between the vertically polarized Nd:YAG pump light at $1.06\mu\text{m}$ and the horizontally polarized output of the semiconductor laser. Tunability was accomplished by replacing mirror M_2 with a prism and rotating either the prism or one of the mirrors.

(2) Tunability--A line width as small as 0.015 nm without any linewidth narrowing elements was observed and was reduced to 0.006 nm by introducing a prism into the cavity. The full tuning range with this prism is 2.5 nm. Additional tuning can be achieved by changing the crystal temperature from 85K to 140K and resulting in a change of the wavelength at the rate of (0.14 nm/K).

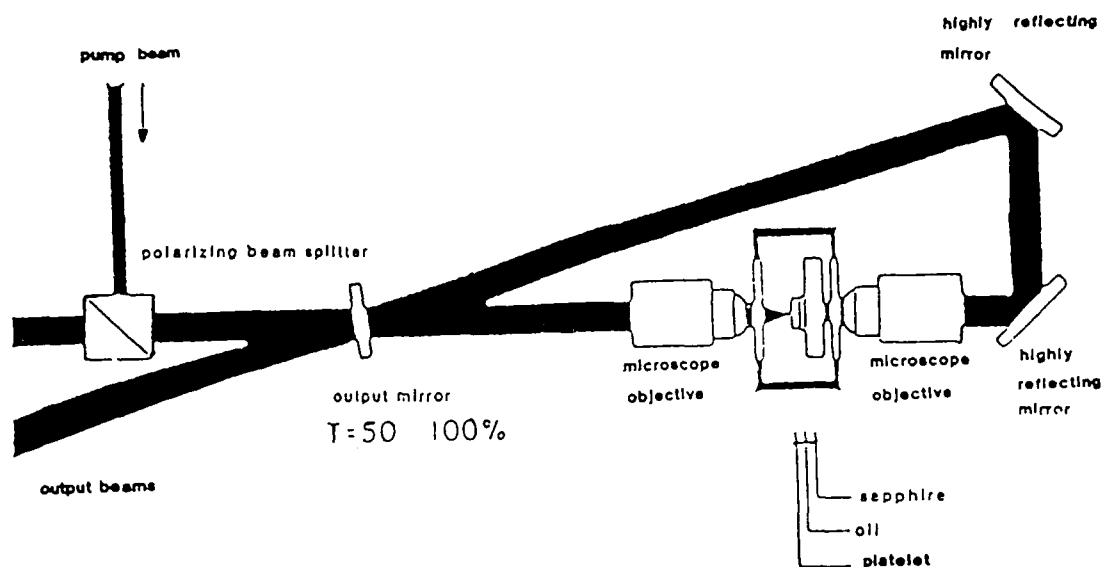


Figure 1. Semiconductor Ring Laser

CW powers of up to 30 mW in each of the two output beams can be obtained by using an output coupler with 8 percent transmittance. Using an output coupler with 30 percent transmittance, a maximum power of 20 mW per beam is measured with a slope efficiency of 15 percent and a power conversion efficiency of 10 percent in the TEM_{00} mode. Lasing was also accomplished using an output coupler with transmittance as low as 50 percent. Coupling back one of the output beams with a retroreflecting mirror results in an output power of more than 50 mW in a single beam. However, in contrast to dye ring lasers, there was no significant increase in the ratio of the powers in the two directions.^[1,2]

(3) Optical Diode--In earlier work with CdS, an attempt was made to operate the ring laser unidirectionally. An optical diode^[3, 4] consisting of a Faraday rotator and a crystalline quartz half-wave plate was built for this purpose. The optical diode provides a 33° polarization rotation and a differential loss of ~ 0.30 . To ensure that after rotation the vertically polarized component of the beam is ejected from the cavity, polarizing beamsplitters were placed inside the cavity (Figure 2).

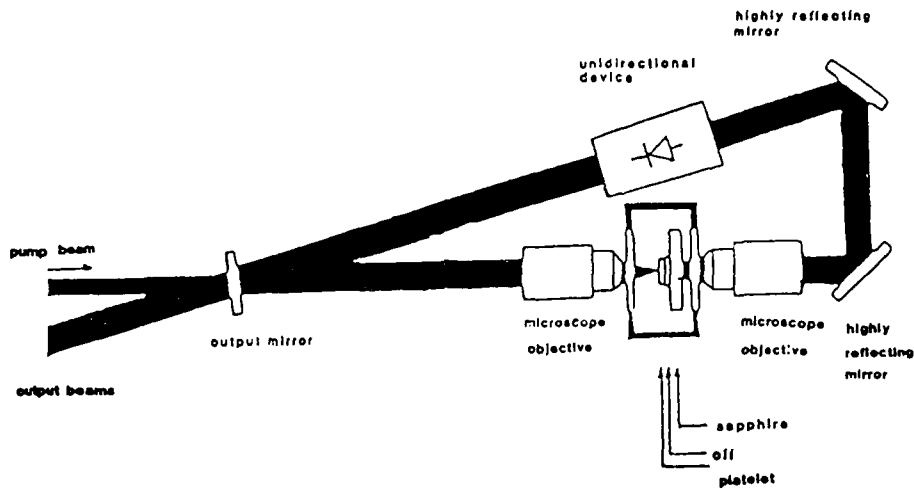


Figure 2. Semiconductor Ring Laser with Optical Diode

A unique feature of the semiconductor laser lies in the Fabry-Perot etalon formed by the faces of the crystal providing an optical diode by itself. This effect is produced by the unequal reflectivities of the two faces, combined with gain in the medium in between. The reflectivities (0.21 and 0.06) are unequal because of the asymmetrical mounting of the platelet. The differential reflection loss of the Fabry-Perot can be as high as 0.50 at net gain in the platelet of 1.8 with virtually no reflection for the counterclockwise (ccw) propagating beam.

We have found that the optical diode formed by the Fabry-Perot (FP) of the platelet is stronger than the optical diode formed by the Faraday rotator (FR) and half-wave plate.^[5] A ratio between ccw and clockwise (cw) beam intensities as high as 5 are observed when both optical diodes are set to favor the ccw beam. The ratio is decreased to 2 when the preferred direction of the FP diode is reversed. Under all circumstances the lasing threshold for CW and ccw beams is exactly the same, as is the wavelength.

A single-layer AR coating on the vacuum side of the $\text{PbS}_{1-x}\text{Se}_x$ platelet should greatly attenuate the FP diode effect. In this case, the direction of the strongest beam should follow the FR diode with a ratio of about 1.5.

That the strongest beam never takes over completely, even though gain competition takes place in the gain medium, can be explained by the theory of two coupled oscillators.^[3] This predicts an increase in coupling if suppression of one of the beams is attempted.

(4) Beam Quality--Outside the beam waists, which are located at the platelet and between M_1 and M_3 , reflection from flat surfaces will be divergent. Also, since all components are AR coated and slightly tilted, coupling through reflection other than from the platelet is not likely to occur. Therefore, the cavity is tilted up to 12° in an attempt to eliminate the coupling. To make this possible, doublets were used instead of microscope objectives with little change in performance. When the dewar is tilted, however, the beams should still go perpendicular to the platelets, thereby going off-axis through the doublets. Forcing the beam to the center by means of an iris increases the lasing threshold for both beams beyond damage threshold before coupling is eliminated.

In order to check that no nonlinear effect was involved in the reflection, a pump-probe experiment using a second pump laser as probe was performed. No evidence of enhanced or nonperpendicular reflection when pumping the platelet was found. This excludes a possible explanation for the coupling between the two beams by degenerate four-wave mixing involving two transverse beams in the plane of the platelet.^[6]

(5) Comparison with Color-Center Lasers--The most singular feature of the semiconductor lasers being discussed is that we are not dealing with gain centers (atoms, ions, molecules, complexes) sparsely distributed in a passive medium or empty space, but rather with the problem of inverting the atoms in an entire block of solid, unlike any other kind of laser. In case of color center lasers, the emission IR ($1\ \mu\text{m}$ to $4\ \mu\text{m}$) occurs between defect states in an ionic crystal. This restricts operation to low temperatures because of thermalization of the defects; in fact, the crystal must often be liquid nitrogen cooled at all times to avoid center reorientation. In addition, orientational bleaching reduces crystal effectiveness, and crystals are difficult to produce. Although F_2^+ centers

with long room temperature shelf lives are now being developed, these lasers still pose considerable practical difficulties.

Semiconductor lasers provide the potential for the generation of repetitive pulses tunable over a very wide range. The proposed lasers presented here operate continuously, which can be a considerable advantage in many applications. Semiconductors have practical advantages over F-center lasers in terms of availability and shelf life. In unmode-locked operation, very narrow linewidth operation may be possible, perhaps narrower than dye lasers. Optically pumped $\text{PbS}_{1-x}\text{Se}_x$ semiconductors should provide a useful source for a variety of applications in both the time and frequency domains.

II. DESIGN DETAILS

1. CRYSTAL GAIN MEDIA

The $\text{PbS}_{1-x}\text{Se}_x$ laser samples were grown in laboratories using the Bridgeman technique with nominal compositions of $X = 0, 0.2, 0.4, 0.6, 0.8$, and 1.0 are available. Wafers with $\{1\ 0\ 0\}$ surfaces were mechanically and then chemically polished to a thickness of about 30μ and subsequently cleaved along $\{1\ 0\ 0\}$ planes to obtain a proper cavity. For each alloy composition lasers were prepared for both n- and P-type crystals (free carrier concentration between 2×10^{17} and $6 \times 10^{18} \text{ cm}^{-3}$). In experiments involving other II-VI compounds, no systematic dependence of the spontaneous or stimulated output on the conductivity or carrier concentration was found. Since these crystals almost blanket the wavelength region from $3\ \mu\text{m}$ to $5\ \mu\text{m}$, it is clear that only a small number of properly selected compositions would be needed to completely cover this region.

a. Graded Bandgap Structures--A new technique which allows a large range in wavelength tunability of the resonator output was explored. This can be achieved in principle by forming an array of crystals with different bandgaps next to each other or by growing a crystal or set of crystals that have a graded bandgap from one side of the crystal to another. This should allow a much larger range in wavelength tunability than can be achieved by a semiconductor with a single uniform bandgap. As a result, a much larger range of output wavelengths can be covered.

Because these platelet lasers have a very long shelf life and do not suffer from photochemical damage, the active medium will last much longer than dye or F-center lasers. In addition, the technique is compatible with automated wavelength scanning. While during the course of this research, no crystal with graded bandgap structure was grown, we have nevertheless, examined the concept of such a structure and its use in our cavity. Figure 3 shows the proposed concept. M_1 and M_2 are mirrors of the laser cavity, L_1 and L_2 are lenses to collimate the fluorescence from the pump radiation. The sample, S , is pumped through lenses L_4 and L_3 by a pump beam. The sample, S_1 , is mounted on a heat sink, HS, and housed in a closed chamber indicated by C. The sample may be formed by a stacked array of crystals with varying bandgap(s) as shown in Figure 4. For a

set of n crystals, each having a different bandgap, the crystal may be mounted so that the bandgap semi-continuously varies from the top to the bottom of the stack.

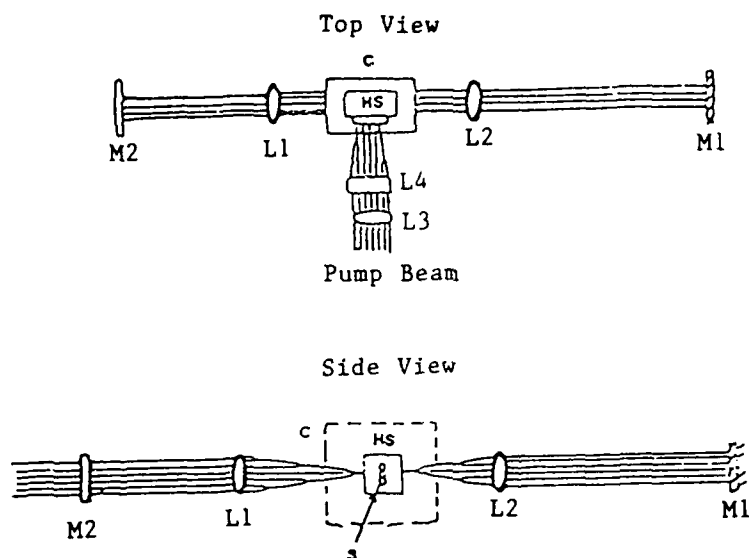


Figure 3. Schematic Diagram of Graded Bandgap Structure

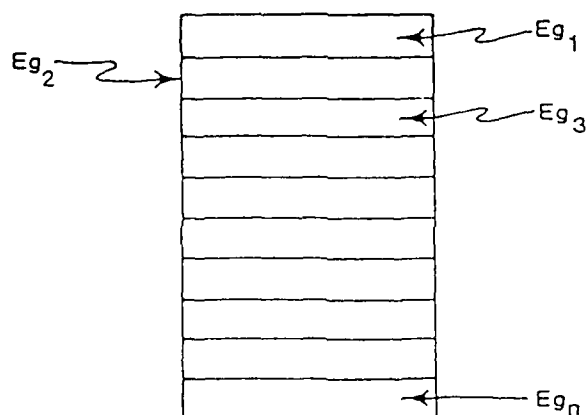


Figure 4. Stacked Array of Crystals

As an example, if the samples are S_1 through S_{11} then for a $\text{PbS}_{1-x}\text{Se}_x$ crystal:

S_1	=	PbS
S_2	=	$\text{PbS}_{0.9}\text{Se}_{0.1}$
S_3	=	$\text{PbS}_{0.8}\text{Se}_{0.2}$
S_4	=	$\text{PbS}_{0.7}\text{Se}_{0.3}$
S_5	=	$\text{PbS}_{0.6}\text{Se}_{0.4}$
S_6	=	$\text{PbS}_{0.5}\text{Se}_{0.5}$
S_7	=	$\text{PbS}_{0.4}\text{Se}_{0.6}$
S_8	=	$\text{PbS}_{0.3}\text{Se}_{0.7}$
S_9	=	$\text{PbS}_{0.2}\text{Se}_{0.8}$
S_{10}	=	$\text{PbS}_{0.1}\text{Se}_{0.9}$
S_{11}	=	PbSe

It seems feasible to grow a single crystal such that the bandgap continuously varies from one side of the crystal to the other. Figure 5 exhibits a situation where at point A the crystal has a bandgap of E_A and at point B the crystal has a band gap of E_B ; this can be continuously varied during the growth process. Examples include ternary compounds such as $\text{PbS}_x\text{Se}_{1-x}$. If x is continuously varied during the growth process, then the bandgap will change from one side of the crystal to the other. Since the bandgap of these crystals ranges from approximately 4 eV to 0.1 eV, a very large tuning range in wavelength is possible, i.e., 0.3 μm to 10 μm , utilizing a Nd:YAG laser as a pump source.

Figure 6 shows a longitudinally pumped configuration involving stacked array or graded bandgap crystals. In this configuration the coarse tuning is achieved by the mechanical movement of the sample holder. Thus the sample itself is moved up and down to shift from one bandgap region to another, and brings itself into focus with the Nd:YAG pump laser.

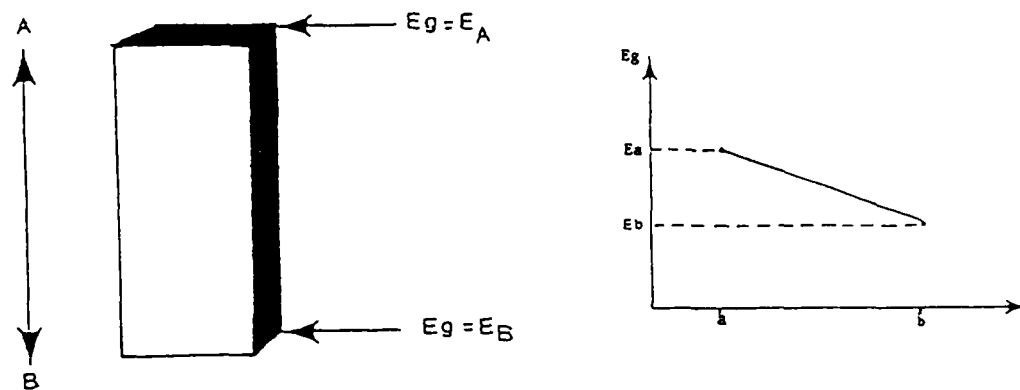


Figure 5. Continuously Varied Bandgap

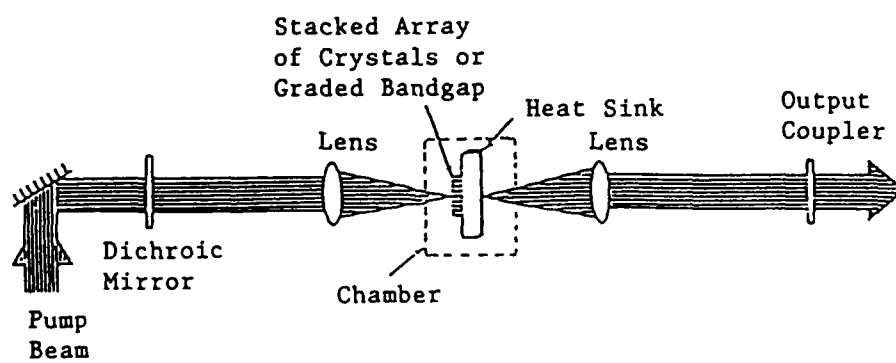


Figure 6. Longitudinally Pumped Variation

If fine tuning of the laser output is desired, then a prism or other frequency selective elements such as grating or Lyot filters may be used as illustrated in Figure 7.

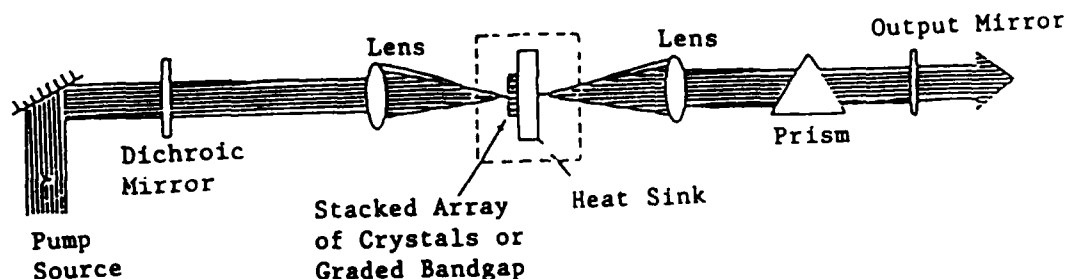


Figure 7. Lyot Filters for Frequency Selective Elements

Similar systems can be developed using transverse pumping as illustrated in Figure 8. The pump beam is focused on the crystal in such a way that the luminescence is transversely emitted and captured by two collimating lenses in the ring cavity. In order to make this possible, the C-axis of the crystal should be oriented horizontally. Then its fluorescence, which primarily has $E \perp c$, will be polarized perpendicularly to the vertically polarized pumped beam.

This technique, if successful, can be one of the unique characteristic features of the semiconductor laser system. First of all, the system can operate at a wavelength region where dye lasers and F-center lasers cannot operate, and secondly, it is unlike dye lasers where the change of dye circulators and dye cells requires substantial cleaning of the entire system which involves a very inconvenient and time consuming process.

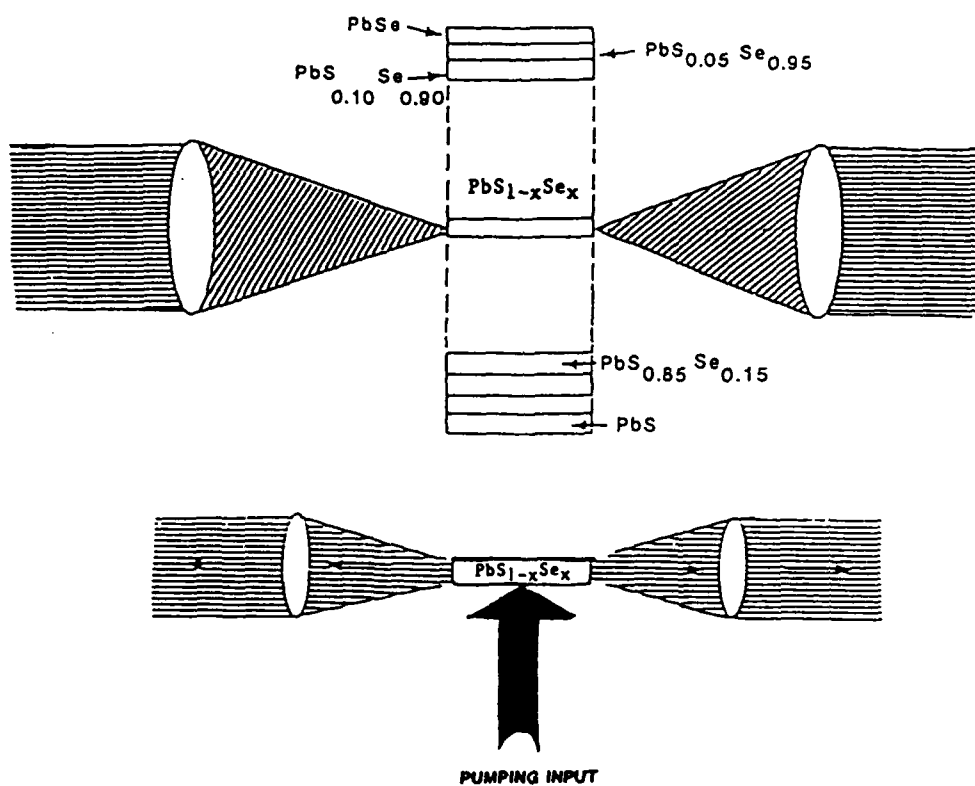


Figure 8. Transverse Pumping

2. CW AND PULSED OPERATION OF THE $\text{PbS}_{1-x}\text{Se}_x$ LASER UNDER A VARIETY OF PUMPING CONFIGURATIONS AND SOURCES

a. CW and Pulsed Output Characteristic--The samples in the ring resonator were pumped by a Nd:YAG laser (Quantronix model 416) at $1.06\text{ }\mu\text{m}$ which was already operating in the laboratory. The samples were excited with either a CW, mode-locked, or Q-switched Nd:YAG laser operating at $1.06\text{ }\mu\text{m}$. The TEM_{00} output of the pump was focused into the sample and the output of the resonator (laser emission) was monitored by a grating spectrometer and detected by a Ge:Cu photo conductor.

b. CW Operation--The Nd:YAG laser, at $1.064\text{ }\mu\text{m}$, operating continuous wave in the TEM_{00} mode (Quantronix model 416 in the laboratory) delivering up to 20 watts, was utilized as a pump source. The spontaneous emission spectra with and without the external cavity was examined. An increase in power by a factor of at least 5000 when the external resonator is aligned (compared with the spontaneous emission output) and the linewidth should narrow down to less than 0.1 nm without any frequency selective elements in the cavity. A threshold lasing condition as low as 100 KW/cm^2 using a 92 percent reflecting output mirror was expected; the threshold can be raised but the output power should increase considerably. Under normal pumping configuration with 1 watt of CW pump power incident on the crystal, we estimate 97 mW CW output at $3\text{ }\mu\text{m}$ to $5\text{ }\mu\text{m}$ range. This 10 percent power conversion efficiency can be obtained down to 40 mW pump power. This estimate is based upon earlier work on other II-IV materials and the efficiency assumed here is much lower than the best possible from this laser. Calculations show^[6] that if the reflection losses in the microscope objective were reduced from its current 7 percent per pass to a degree that these losses are eliminated and the output coupling is improved, then the output conversion efficiency should be increased to at least 27 percent. An AR-coated "best form" singlet lens was employed to achieve lasing. In the past, this has not been successfully achieved with a singlet lens because of the excessive spherical aberration. However, recent work at TACAN Corporation showed that this chromatic aberration can be compensated for by using a slightly different pump beam.

c. Pulsed Operation of the $\text{PbS}_{1-x}\text{Se}_x$ --Using the Q-switched Nd:YAG laser at 1.064 μm , KHz repetition rate, μsec optical pulses, the $\text{PbS}_{1-x}\text{Se}_x$ laser characteristics were calculated. In the calculations, the approximated position of the quasi-Fermi level for holes during optical excitation of an n-type crystal was utilized. (The calculations for p-type samples would be analogous.)^[7] For a 100-watt peak pulse of pump light focused to a $5 \times 100 \mu\text{m}$ line image (typical experimental values), the excitation level expressed as an equivalent current density is $\sim 6 \times 10^4 \text{ A/cm}^2$. To calculate the carrier density produced by the pump pulse, it is necessary to assume an excess carrier lifetime^[8] of 2 ns and effective carrier confinement to a diffusion region of $\sim 30 \mu\text{m}$. (The excess carrier lifetime is determined to be less than 40 ns from measurements of the spontaneous luminescence decay time.)^[8] Since the excess carrier density $\delta p = \delta n = 2.5 \times 10^{17} \text{ cm}^{-3}$ far exceeds the effective mass density of states, the relation may be used

$$\delta p = N v F_{1/2}(\phi_p) \quad (1)$$

in its degenerate approximations

$$\phi_p = \frac{2.16 \times 10^{-14} (\delta p)^{2/3}}{(m_h/m_0)} \text{ eV} \quad (2)$$

to calculate how far the hole quasi-Fermi level ϕ_p moves into the valence band during the excitation pulse. Mass anisotropy, nonparabolicity, etc., can be neglected as they do not significantly alter the conclusions. For PbS, $m_h \approx 0.1 m_0$ ^[9,10] and we calculate $\phi_p \approx 8.6 \text{ meV}$. Assuming only k-conserving transitions occur, the bandwidth will be given by twice the penetration of the quasi-Fermi level or $\Delta v \sim 17.2 \text{ meV} \approx 140 \text{ cm}^{-1}$. For PbSe $m_h \approx 0.068 m_0$ ^[9,10] and the calculated bandwidth is $\sim 210 \text{ cm}^{-1}$. These numbers, although not expected to be more than rough estimates, do agree with the experimentally observed values of $\sim 200 \text{ cm}^{-1}$. We can conclude that in these optically pumped samples, the bandwidth is probably controlled by the density of excited excess carriers and the extent to which the minority carrier quasi-Fermi level moves into its respective band. While the contribution to the linewidth from indirect transitions (i.e., non-k-conserving) in heavily doped samples could be significant, it apparently

does not dominate at the high pumping levels for our experiments. This is a basic difference between the II-VI from those in III-V compounds, where the linewidths are controlled by the majority carrier density.^[11]

We have followed the work of the late Dr. W. Lo of General Motor Research Laboratories who, along with his colleagues at G.M., pioneered the technology of $\text{PbS}_{1-x}\text{Se}_x$ diode laser.^[12] In comparison with their diode lasers the external cavity source offered much higher output power. We have, however, utilized their temperature stabilized $\text{PbS}_{1-x}\text{Se}_x$ diode laser and injection locked it into our external $\text{PbS}_{1-x}\text{Se}_x$ cavity to achieve transform limited optical pulses at the Nd:YAG laser repetition rate (KHz). The $\text{PbS}_{1-x}\text{Se}_x$ diode lasers are operated at much lower current densities, $\sim 500 \text{ A/cm}^2$, hence the injected carrier density (and the resulting bandwidth) should be much smaller than for the optically pumped case. If a sufficiently high injection level could be reached in a diode, an increase in bandwidth should be obtained; conversely, an optically pumped sample with lower threshold should exhibit a smaller bandwidth. This has been observed in optically pumped samples of other II-VI compounds with thresholds of less than 1 W. In TACAN's configuration the $\text{PbS}_{1-x}\text{Se}_x$ output excludes a few watts of peak power, with μsec pulses of a few KHz repetition rate.

d. Tunable Mode-Locked $\text{PbS}_{1-x}\text{Se}_x$ Laser (3- μm to 5- μm) Pump Sources

(1) The Mode-Locked Nd:YAG Laser at 1.064 μm for Pumping $\text{PbS}_{1-x}\text{Se}_x$ --The Nd:YAG laser, at 1.064 μm , operating continuous wave in the TEM_{00} mode at the 10-20 watt level has been a reliable industrial tool for years. Modifications to this basic system are, of course, required to produce short, stable mode-locked pulses. The convenient 100-MHz pulse repetition rate necessitates the design of an approximately 1.5-meter optical resonator. Elimination of etalon effects requires that all optical surfaces, both intra- and inter-cavity must be wedged with respect to each other. Even with these changes the insertion of an acousto-optic, standing-wave mode-locker into the cavity, it is possible to achieve average mode-locked powers of 10 watts from our Nd:YAG systems. The output of the laser pulses has been measured and using the SHG autocorrelation traces of $\sim 80 \text{ psec}$ has been found to be consistent with the photodiode and sampling head measurements.

Achievement of such performance from a YAG system can no longer be considered routine. Aided by water-cooled, acousto-optic modulators with low acoustic Q, highly-stable RF frequency sources, and invar-stabilized optical resonators, the systems run unattended for hours.

The peak pulse power of greater than one kilowatt produced by a Nd:YAG system which is mode-locked only, can be significantly magnified by simultaneous Q-Switching. The additional acousto-optic element, now a traveling acoustic wave Q-switch, can be added intracavity with little, if any, reduction in average power performance. By fine adjusting the active loss per pass generated by the Q-switch pulses or, as is more frequently the case, allowed to pre-lase at a level just above threshold prior to Q-switch, the laser can be maintained below oscillation at a level just above threshold prior to Q-switched pulse emission. In this latter case, the mode-lock modulator, which runs continuously, is able to fully establish mode-locked conditions, i.e., the mode-locked pulse widths are brought to their minimum value during the time before the growth of the Q-switched pulse. In this way, a train of mode-locked pulses is produced under a Q-switched pulse envelope with FWHM about 300 nsec. Enhancement ratios close to 1000 have been achieved, meaning that peak pulse powers at the peak of the Q-switched pulse envelope are one megawatt. Repetition rates for this minimum pulse width, high peak power operation can range from 0 to 800 Hz. If trains of subnanosecond, lower peak power, mode-locked pulses will suffice, then the laser can be brought below threshold between Q-switched pulses and operated to frequencies beyond 10 kHz.

e. Synchronous Pumping of the $\text{PbS}_{1-x}\text{Se}_x$ Laser with 3- μm to 5- μm Wavelength Span--The application of synchronous pumping by the mode-locked Nd:YAG laser to $\text{PbS}_{1-x}\text{Se}_x$ should result in the generation of tunable picosecond pulses with several watts of average mode-locked power at 100 MHz repetition rate. If desired, the resultant pulses can be cavity dumped at a few KHz repetition rate.

The cavity configuration used for mode-locked operation of the semiconductor laser is very similar to the CW configuration, except the Nd:YAG laser pump is mode-locked to produce a train of 80 ps long pulses at a 100 MHz repetition rate. The semiconductor laser cavity length is set so that the round trip travel time of photons inside the cavity is 10 ns. This equals the time between the incoming Nd:YAG pump laser pulses.

This method of mode-locking is known as synchronous pumping, and it has been used to generate highly repetitive picosecond pulses from semiconductor lasers in the 0.35- μm to 1.7- μm range.^[13] Commercially available sync-pump dye laser systems can

produce pulses less than 1 ps long. The pump pulses provide a "window" of high gain for the semiconductor laser pulses. If the cavity length is properly matched, a short pulse inside the cavity will experience gain on every round trip.

If the semiconductor laser pulse has sufficient power, it will deplete the gain and provide an additional pulse-shortening mechanism. This gain depletion is the reason why pulses much shorter than the pump pulse can be obtained. The theory of synchronously pumped mode-locking is fairly well understood for dye lasers; and the theory has been extended to optically pumped semiconductor lasers in external cavities.^[14]

In previous experiments, pulses as short as 3 ps have been observed using other II-VI and III-V platelets. Output powers higher than 50 mW have been obtained. These techniques can also be extended to $\text{PbS}_{1-x}\text{Se}_x$ crystal platelets. Birefringent filters and etalons can be inserted into the cavity for tuning.

The process of mode-locking changes the output power in a way which might not necessarily be linear. As the input power is varied, the timing advance given to the semiconductor laser pulse should change. This is compounded by the fact that the gain does not vary linearly with the excited state density in a semiconductor. Also, the amount of gain depletion should change; this can also change the conversion efficiency.

f. Effect of Dispersion--One substantial difference between semiconductors and dyes is the strong dispersion present in the semiconductor crystal. Dispersion has been observed to cause pulse spreading in mode-locked dye laser^[15] and solid-state lasers previously, and is the cause of the excess bandwidth observed in the current system.

The pulse chirping in $\text{PbS}_{1-x}\text{Se}_x$ laser is examined, using an experimental set up shown in Figure 9. The output from the $\text{PbS}_{1-x}\text{Se}_x$ laser is sent into the autocorrelator and through a SHG crystal to generate the second harmonic. The second harmonic beam, however, is routed through a 0.5m monochromator rather than directly into a Ge:Cu photo detector. This allows discrimination between the different wavelength components of the pulse.

A chirped pulse^[16] shown schematically in the inset of Figure 9. The wavelength of the pulse is longer at the front end than at the back. This red-to-blue chirp would be expected from a normally dispersive element. The monochromator can be

used to determine if the pulse is chirped by selecting a portion of the pulse bandwidth. For a chirped pulse, that portion will have a narrower autocorrelation trace. If the monochromator is tuned to the center of the second harmonic line, the entire pulsewidth is observed because the red portion of the pulse can interact with the blue portion to create second harmonic at this wavelength.

g. The Effects of Anti-Reflection Coating--The $\text{PbS}_{1-x}\text{Se}_x$ crystals can be coated with an anti-reflection (AR) coating to reduce the effect of the crystal Fabry-Perot and thereby increase the cavity bandwidth. The coating should also improve the performance of the thicker crystal. To produce more Fourier limited pulses, bandwidth limiting elements can be inserted into the cavity. Both a birefringent filter and a Fabry-Perot etalon can be used in our present $\text{PbS}_{1-x}\text{Se}_x$ laser.

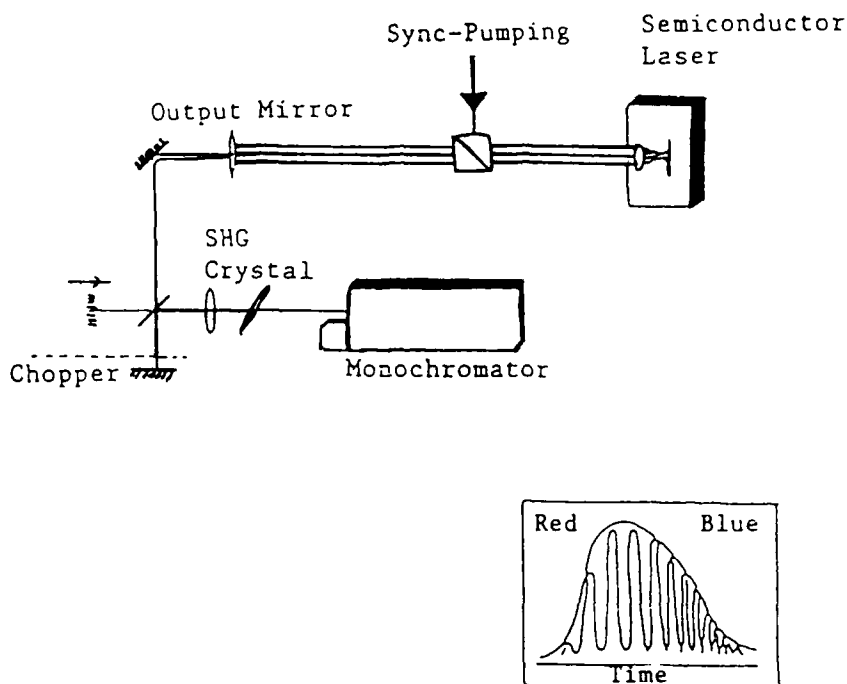


Figure 9. Experimental Setup of Pulse Chirping

3. EXPERIMENTAL SETUP

The optical configuration used in our experiment is shown in Figure 10. The lead salt materials, of 3 to 4 μm thickness, were grown of BaF_2 substrates. The growth method and film characteristics are similar to those reported previously.^[22] The high-reflective mirror of the cavity was coated directly on the lead salt materials, and these substrates were finally adhesively bonded to the copper cold finger of a cryogenic vacuum dewar. The temperature of the cold finger was measured by means of a silicon diode (Lake Shore Cryotronics, Inc.) which was mounted in a hole drilled behind the sample.

The pump source was a mode-locked Nd:YAG laser (Quantronix 416) at a wavelength of 1.06 μm , 100 MHz pulse repetition rate and a pulse width of 100 ps FWHM. In order to optically isolate the pump laser from the lead salt laser resonator, we used an acousto-optic modulator (AOM), which at the same time served as a continuously variable attenuator. The pump power was monitored with a fast photodiode and a sampling oscilloscope while the generated laser radiation was measured with an InSb photodetector.^[27-29]

The pump beam was focused on the sample with a well corrected zinc selenide doublet. The focal lengths at 1.06 μm and 4.1 μm were 29 mm and 30 mm, respectively. The difference in focal lengths between 4.1 μm and 4.8 μm was approximately 0.05 mm. To compensate for the large chromatic aberration between the pump wavelength and the generated wavelengths, it was necessary to use a telescope assembly which caused the pump beam to be diverging as it entered the objective. The telescope was designed to create a 0.7-mm beam waist at a distance of approximately 0.7 m before the objective. Assuming a Gaussian pump beam cross section, the calculated $1/e^2$ spot size on the sample was about 14 μm .

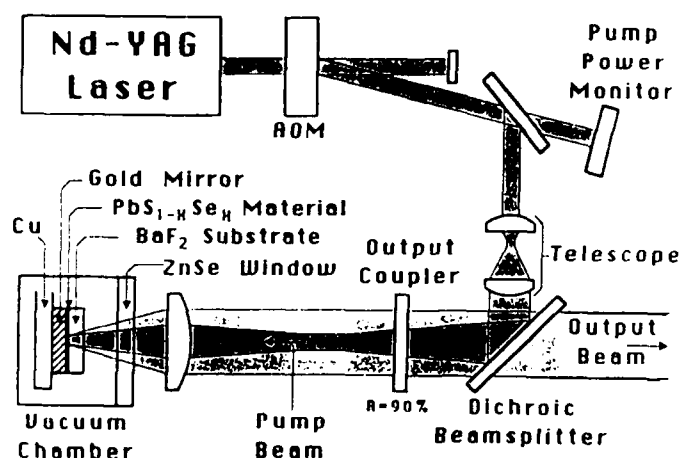


Figure 10. Experimental Configuration

4. EXPERIMENTAL RESULTS

The sample was cooled by use of liquid helium, which kept the temperature of the cold finger at approximately 8K. At this temperature we achieved cw mode-locked lasing above a threshold average power of 25 to 35 mW. Figure 11 shows the input versus output power characteristics. The average output power was estimated from the known responsivity (2A/W) of the InSb detector. Using this value we achieved a maximum average power of 1 mW at the wavelength of 4.1 μm and 0.6 mW at 4.8 μm . By increasing the input power we found that the corresponding output power reached a saturation point and then started to decrease. This is most likely due to local heating of the sample. The possibility of permanent damage as a cause for this saturation can be ruled out since it was possible to repeat the readings in Figure 11.

We also operated the lead salt laser at elevated cold finger temperatures up to 150K. However, it was not possible to run the laser cw mode-locked at temperatures above about 50K. At such temperatures, it was always necessary to use a beam chopper to decrease the average pump power so as to maintain lasing action. At $T=78\text{K}$ the lasing ceased when the chopper gate time was longer than a few μs (see insert in Figure 11).

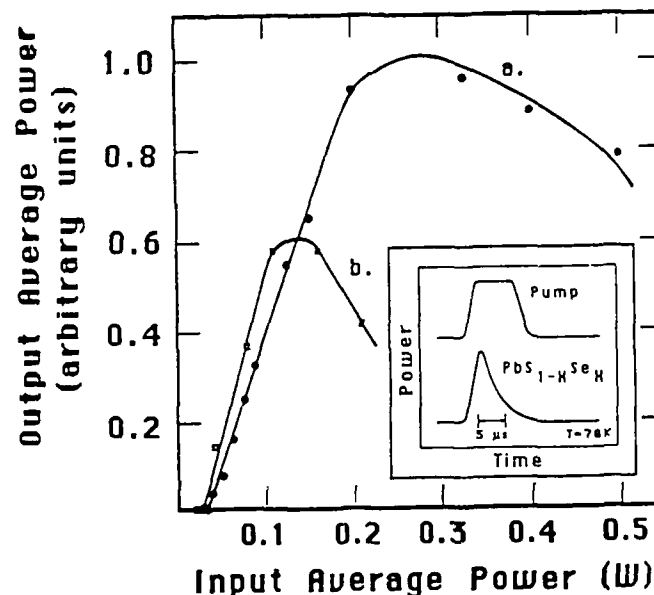


Figure 11. Input-Output Power Characteristics at a Cold Finger Temperature of 8K
 - a. and b. correspond to the materials $x=0$ and $x=0.3$
 - The insert shows the pump power and the $\text{PbS}_{1-x}\text{Se}_x$ laser power versus time at a temperature of 78 K.

The spectrum of the output beam was measured with a grating blazed at $4.0\ \mu\text{m}$. Figure 12 shows the spectra of the two samples recorded at an input power of 200 mW and a temperature of 8K. The resolution of the monochromator was 3 nm in our experiment. The sample $x=0$ exhibited multiple peaks as opposed to the sample $x=0.3$, which showed one single peak in its spectrum. This discrepancy is attributed to the difference in free spectral range of the substrates. Sample $x=0$ had a BaF_2 substrate of thickness 0.45 mm while the $x=0.3$ material had a BaF_2 substrate of thickness three times larger. With the resolution of our monochromator, it was only possible to resolve the substrate Fabry-Perot modes of sample $x=0$. Anti-reflection coating of the substrate would eliminate the Fabry-Perot modes displayed in Figure 12.

We also operated the laser with a single-element, best shape, intracavity lens. Even though it was possible to reach the threshold for oscillation, the aberrations introduced by the single lens gave rise to very large round trip losses, resulting in a resonator with low Q-value and low output power. The low Q-value was also displayed by the fact that the laser output power was very insensitive to misalignment of the output coupler. This can be expected in a resonator where the photons, on an average, make few round trips. With the diffraction limited doublet, the output power was more sensitive to axial misalignment of the output coupler. We found that the generated power decreased to half its maximum value when the resonator length was changed by $\pm 0.7\ \text{mm}$ about its optimum length. Diffraction-limited optics are therefore crucial for the resonator configuration used.^[30-32]

We did not measure the width of the generated laser pulses due to the lack of appropriate equipment. However, from other experiments on optically pumped semiconductor lasers we would expect the $\text{PbS}_{1-x}\text{Se}_x$ laser pulses to have durations on the order of 10 ps.

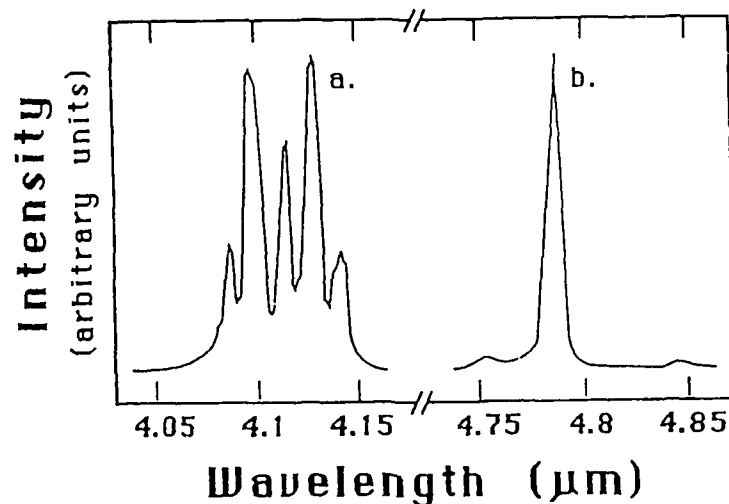


FIGURE 12. Spectral Characteristics at 200 mW Input Average Power.
a. and b. show the spectrum for $x=0$ and $x=0.3$, respectively

a. Exploration of Room Temperature Operation Utilizing Superlattice Structure--We were interested in extending the operation of the present $\text{PbS}_{1-x}\text{Se}_x$ laser to room temperature. However, success was made only up to an elevated temperature of 150K. In such a situation involving 50K it was necessary to chop the pump beam in order to maintain lasing. There are many problems inherent in the design of the optically pumped semiconductor laser and these problems are somewhat distinct from those of other lasers. At low temperatures, electrons and holes created in direct bandgap semiconductors can recombine to form excitons which are no longer bound to neutral impurities. Thus, the luminescence becomes much stronger (only at low temperature above 50K) in the emission spectrum. In GaAs, for instance, the exciton-phonon coupling and thus the relative strength of the luminescent lines change with temperature as well. The bandgap shifts toward the red as the temperature is increased and the linewidth of the emission broadens. This variation of the emission wavelength with temperature is useful for the tuning of semiconductor lasers. Unfortunately, the radiative efficiency decreases as temperature increases, and most semiconductor lasers operate only at temperatures around 100K or below. The low temperature operation and the very tight focus requires that the focusing optics be placed inside the cooling chamber close to the sample. The sample must be held very rigidly inside the chamber while it is also mobile to allow cavity alignment and movement from sample to sample.

(1) Room Temperature $\text{PbS}_{1-x}\text{Se}_x$ Laser--A solution to the problem of tight focusing optics and sample movement as demonstrated in the ring cavity semiconductor laser design has been found. With new development in the growth of $\text{PbS}_{1-x}\text{Se}_x$ superlattice structures, linear absorption measurements have demonstrated distinct excitonic peaks at room temperature--this is because the confinement increases exciton binding energy without increasing LO phonon coupling. The strong and readily saturable superlattice excitonic absorption at room temperature should have a major impact in room temperature operation of these lasers, thus allowing room temperature devices to be fabricated with materials and switching intensities compatible with laser diode sources. Because superlattice material is compatible with diode lasers, not only in terms of growth technology, but also in terms of light wavelength and power levels, the possibility of using such quantum well material at room temperature in an external ring cavity pumped by a commercially available diode laser as the sole light source has been explored. Because of the exceptionally strong absorption resonances near the bandgap energy due to excitons such $\text{PbS}_{1-x}\text{Se}_x$ quantum well materials were an excellent choice for the scheme.

(2) Lead-Salt Quantum Well Structures--Recent advances in lead salt quantum well diode lasers has lead to the construction of devices in the 2.5- μm to 30- μm wavelength range. These devices have previously required cryogenic cooling (100K) for CW operation. The use of quantum well, large optical cavity structures has substantially improved the operating temperatures to 174K CW (at 4.41 μm) and to 260 K pulsed (at 3.91 μm). These structures have a single PbTe quantum well with lattice-matched $\text{Pb}_{1-x}\text{Eu}_x\text{Se}_y\text{Te}_{1-y}$ confinement layers grown by molecular beam epitaxy. The emission energy shifts have been calculated using a finite square well with nonparabolicity effects included. Initial work has also been done on multiple quantum well lasers. The maximum operating temperatures are comparable to those of single quantum well laser, with carrier leakage out of the quantum wells a significant limitation.

III. CONCLUSIONS

In this program, we have successfully demonstrated the first optically pumped tunable semiconductor laser with external cavity in the $3\text{ }\mu\text{m}$ - $5\text{ }\mu\text{m}$ region of the electromagnetic spectra. We have also successfully demonstrated the cw mode-locked operations of the cavity under a synchronously pumped configuration generating picosecond optical pulses in the $3\text{ }\mu\text{m}$ - $5\text{ }\mu\text{m}$ range at a 100 MHz repetition rate.

This $3\text{ }\mu\text{m}$ - $5\text{ }\mu\text{m}$ is a range which is not entirely available from dye lasers. Because of the lack of dye jet fluctuations, these platelet semiconductor lasers provide narrower linewidths than dye lasers, and samples mounted adjacent to each other can be changed easily and quickly to provide tunability over a broad range. Furthermore, a very long shelf-life and the lack of orientation and bleaching makes these lasers more practical than F-center lasers for many applications. The extension of this laser for higher power operation will utilize this tunable semiconductor oscillator as a master oscillator. Higher power output can be achieved in a chain of synchronized amplifiers pumped by the same Nd:YAG laser in a $\text{PbS}_x\text{Se}_{1-x}$ crystals as chains of optical amplifiers involving long pulses, large aperture and high beam quality.

The successful demonstration of this laser should have immediate applications involving infrared communications, spectroscopy, flame diagnostics and testing of infrared optical fibers.

IV. REFERENCES

1. J. M. Green, J. P. Hohimer, and F. K. Tittle, Optics Commun. **7**, 4 (1973).
2. R. Ulrich and H. P. Weber, Appl. Phys. Lett. **20**, 1 (1972).
3. T. F. Johnston and W. Proffitt, IEEE J. Quantum Electronics, **16**, 4 (1980).
4. S. M. Jarrett and J. F. Young, Opt. Lett. **4**, 176 (1979).
5. A. Fuchs, D. Bebelaar, and M. M. Salour, Appl. Phys. Lett. **43**, 32 (1983).
6. M. M. Salour (unpublished).
7. A. Mooradian, A. J. Strauss, and J. A. Rossi, IEEE J. Quantum Electronics, QE-9, p. 347 (1973).
8. This value is consistent with an extrapolation of the photoconductive lifetime measured in much lighter doped Pb-salt photodetectors. For example, I. Melngailis and T. C. Harman, "Single crystal lead-tin chalcogenides," in Semiconductors and Semimetals, R. K. Willardson and A. C. Beer, Eds. New York: Academic Press, vol. 5, p. 166, (1970).
9. K. F. Cuff, M. R. Ellett, C. D. Kuglin, and L. R. Williams, "The Band Structure of PbTe, PbSe, and PbS," Proc. 7th Int. Conf. Physics of Semiconductors, Paris (1964); M. Hulin, Ed. Paris and Dunod. New York: Academic Press, p. 677, (1964).
10. D. L. Mitchell, E. D. Palik, and J. N. Zemel, "Magneto-optical Band Studies of Epitaxial PbS, PbSe, and PbTe," Proc. 7th Int. Conf. Physics of Semiconductors, Paris, (1964); M. Hulin, Ed. Paris and Dunod. New York: Academic Press, p. 325, (1964).
11. H. C. Casey and R. H. Kaiser, "Analysis of n-type GaAs with Electron-beam Excited Radiative Combination," J. Electrochem. Soc., Vol. 114, p. 149, (1967).
12. W. Lo and D. E. Swets, Appl. Phys. Lett. **33**, p. 938, (1978).
13. C. B. Roxlo and M. M. Salour, Appl. Phys. Lett. **38**, 738 (1981); W. L. Cao, A.M. Vaucher, and C. H. Lee, Appl. Phys. Lett. **38**, 306 (1981); A. M. Vaucher, W. L. Cao, J. D. Ling, and C. H. Lee, IEEE Journal of Quantum Electronics, February 1982.
14. C. B. Roxlo, R. S. Putnam, and M. M. Salour, IEEE Journal of Quantum Electronics QE-18, No. 3, 338-342 (1982).
15. G. W. Fehrenbach and M. M. Salour, Appl. Phys. Lett., **41**, 4, (1982).
16. C.B. Roxlow, R.S. Putnam, and M.M. Salour, Proc. SPIE, "Picosecond Lasers and Applications," **38**, 31, (1982).
17. R.S. Putnam and M.M. Salour, Proc. SPIE, "Picosecond Optoelectronics," **439**, 66 (1984).
18. B. Valk, T.S. Call, M.M. Salour, W. Kopp, and H. Morkoc, Appl. Phys. Lett. **49**, No. 3, 119 (1986).

19. A. Mooradian, A.J. Strauss, and J.A. Rossi, IEEE Quantum Electron. QE-9, 347 (1973).
20. W. Gellerman, Y. Yang, and F. Luty, Proc. SPIE, "High Power and Solid State Lasers", 622, 151 (1986).
21. M.M. Broer and L.G. Cohen, J. Lightwave Technology LT-4, No. 10, 1509, (1986).
22. T.K. Chu, A.C. Bouley, and G.M. Black, Proc. SPIE, "Infrared Detector Materials", 285, 33 (1981).
23. C.B. Roxlo, D. Bebelaar, and M.M. Salour, Appl. Phys. Lett. 38, 507 (1981).
24. R.S. Putnam, C.B. Roxlo, M.M. Salour, S.H. Groves, and M.C. Plonko, Appl. Phys. Lett. 40, 660 (1982).
25. R.S. Putnam, M.M. Salour, and T.C. Harman, Appl. Phys. Lett. 43, 408, (1983).
26. W.L. Cao, A.M. Vacher, and C.H. Lee, Appl. Phys. Lett. 38, 653, (1981).
27. J.P. Van der Ziel, in Semiconductors and Semimetals, Vol. 22, Part B, Lightwave Communications Technology, edited by W.T. Tsang (Academic, Orlando, Florida, 1985), Chap. 1.
28. D.C. Reynolds, K.K. Bajaj, C.W. Litton, P.W. Yu, W.T. Masselink, R. Fischer, and H. Morkoc, Phys. Rev. B 29, 7038 (1984).
29. W.T. Masselink, P.J. Pearah, J. Klem, C.K. Peng, H. Morkoc, G.D. Sanders, and Y.C. Chang, Phys. Rev. B 32, 8027 (1985).
30. S.R. Chinn, J.A. Rossi, C.M. Wolfe, and A. Mooradian, IEEE Quantum Electron. QE-9, 294 (1973).
31. R.C. Millier, R. Dingle, A.C. Gossard, R.A. Logan, W.A. Nordland, and W. Wiegman, J. Appl. Phys. 47, 4509 (1976).
32. K. Vilhelmsson, B. Valk, and M. M. Salour, Appl. Phys. Lett. 50, 13, (1987).

END

DATE

FILMED

5-88

DTIC